Electronic Supplementary Information

Identification of active sites for CO_2 hydrogenation in Fe catalysts by first-principles microkinetic modelling

Seung Ju Han[a], Sun-Mi Hwang[a], Hae-Gu Park[a], Chundong Zhang[b], Ki-Won Jun[a], Seok Ki Kim[a,*]

[a]Carbon Resources Institute, Korea Research Institute of Chemical Technology (KRICT), 141, Gajeongro, Yuseong-gu, Daejeon 34114, Republic of Korea

[b]State Key Laboratory of Materials-Oriented Chemical Engineering, College of Chemical Engineering, Nanjing Tech University, Nanjing, Jiangsu 211816, P. R. China

*Corresponding author: skkim726@krict.re.kr

Contents

Table S1. Electronic formation energies of major adsorbents on the Fe carbide and oxide surfaces. 3

Figure S1. The optimized configurations for CO_2 adsorption on Fe-based surfaces. 4

Figure S2. Relative energy diagram for the formation of vacancy site in Fe_5C_2 (001) and Fe_3O_4 (111) surface. Representative structures of clean surfaces and surfaces with vacancy site are shown above the diagram. T = 300 °C and P = 2.5 MPa. 5

Figure S3. The optimized unit cell structures of Fe-based surfaces. 6

Table S2. Elementary reaction steps for RWGS reaction over Fe-based surfaces 7

Table S3. Electronic formation energies and vibrational frequencies of adsorbents on the Fe-based surfaces 8

Figure S4. Formation energies of intermediates and transition states, plotted as a function of CO_2* formation energy (E_{CO2}) and OH* formation energy (E_{OH}). Scaling parameters are given below the plots. 14

Figure S5. Rate volcano plots for elementary reaction steps in RWGS reaction, plotted as a function of the descriptors, CO_2* formation energy and OH* formation energy. T = 300 °C and P = 2.5 MPa. 15

Figure S6. The optimized unit cell structures of Fe_3O_4 (111) and Me-Fe_3O_4 (111) surfaces. In the Me-Fe_3O_4 surfaces, element of Fe_{oct2} site is substituted by V, Cr, Mn, Fe, Co, Ni, Cu, and Zn. 16

Figure S7. Bell–Evans–Polanyi correlations for (a) C-H bond, (b) C-O bond, and (c) O-H bond formation steps on Fe-based surfaces. 17

Table S4. Self-interaction parameters for Fe (110) surface. 18

Table S5. Verification of self-interaction parameters by comparing E_{DFT} and E_{est} at 0.375 ML. 19

Figure S8. CO production rates over Fe (square), Fe_5C_2 (circle), and Fe_3O_4 (triangle) surfaces with various facets plotted as a function of the CO_2* and OH* formation energies. T = 300 °C and P = 2.5 MPa. 20

Table S1. Electronic formation energies of major adsorbents on the Fe carbide and oxide surfaces.

Surface name	Species name	Site name	Formation energy
Fe_3C	CO	Fe	1.154
		C	3.042
	CO_2	Fe	1.839
		C	2.528
	O	Fe	-0.644
		C	2.145
	H	Fe	-0.578
		C	-0.319
Fe_5C_2	CO	Fe	1.351
		C	2.766
	CO_2	Fe	1.863
		C	3.154
	O	Fe	-0.319
		C	1.085
	H	Fe	-0.395
		C	2.817
Fe_3O_4	CO	Fe	1.286
		O	3.334
	CO_2	Fe	1.819
		O	1.411
	H	Fe	0.187
		O	2.668
Fe_2O_3	CO	Fe	1.523
		O	2.521
	CO_2	Fe	2.242
		O	1.289
	H	Fe	0.207
		O	0.299

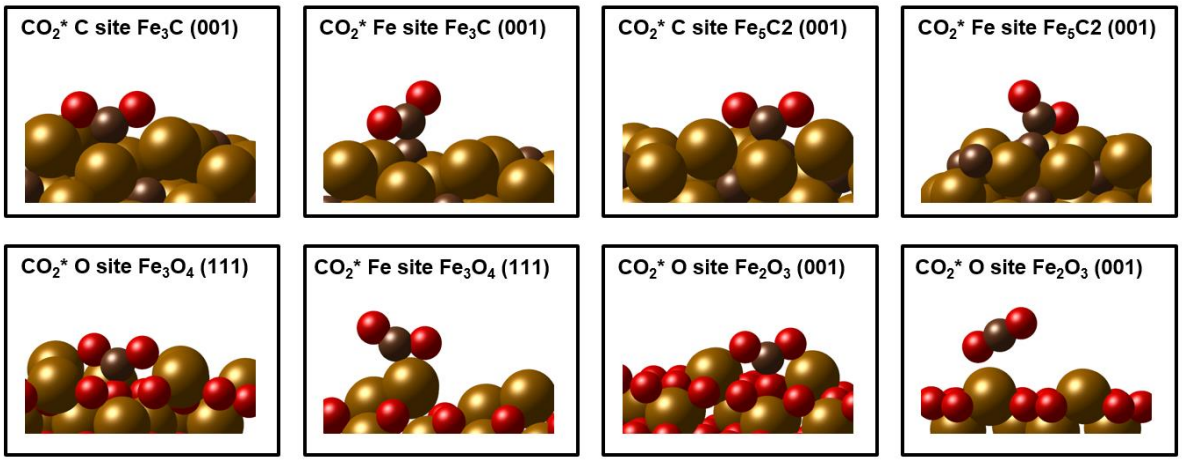

Figure S1. The optimized configurations for CO_2 adsorption on Fe-based surfaces.

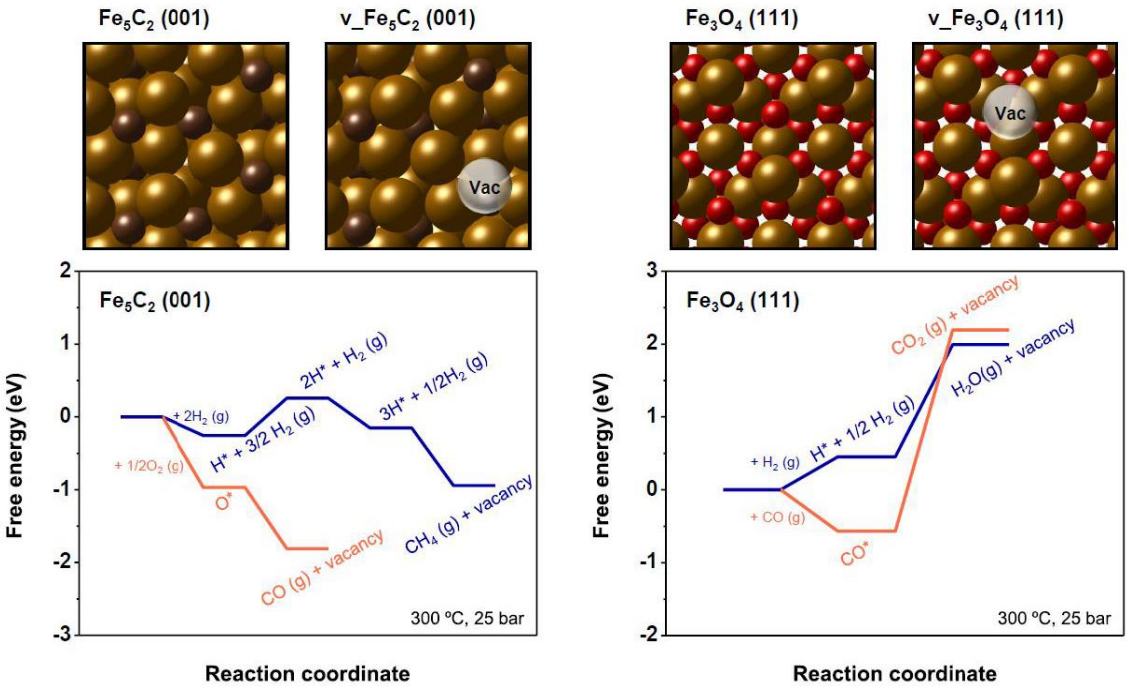

Figure S2. Relative energy diagram for the formation of vacancy site in Fe_5C_2 (001) and Fe_3O_4 (111) surface. Representative structures of clean surfaces and surfaces with vacancy site are shown above the diagram. T = 300 °C and P = 2.5 MPa.

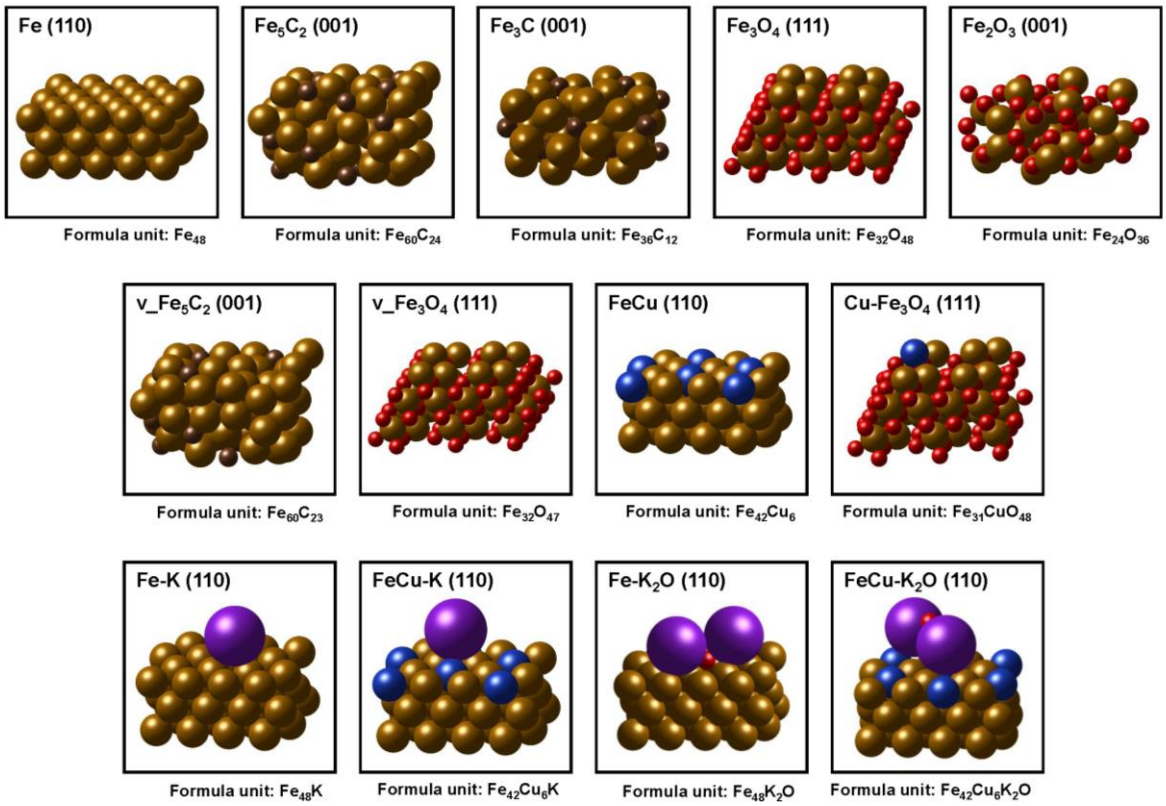

Figure S3. The optimized unit cell structures of Fe-based surfaces.

Table S2. Elementary reaction steps for RWGS reaction over Fe-based surfaces

Elementary step
H_2_g + *_h + *_h → H_h + H_h
CO_2_g + *_s → CO_2_s
CO_s → CO_g + *_s
O_s + H_h ↔ O-H_s + *_h → OH_s + *_h
OH_s + H_h ↔ H-OH_s + *_h → H_2O_g + *_s + *_h
CO_2_s + *_s ↔ CO-O_s + *_s → CO_s + O_s
CO_2_s + H_h ↔ COO-H_s + *_h → COOH_s + *_h
CO_2_s + H_h ↔ H-COO_s + *_h → HCOO_s + *_h
COOH_s + *_s ↔ CO-OH_s + *_s → CO_s + OH_s
HCOO_s + *_s ↔ HCO-O_s + *_s → CHO_s + O_s
CHO_s + *_h ↔ H-CO_s + *_h → CO_s + H_h
COOH_s + H_h ↔ H-COOH_s + *_h → HCOOH_g + *_s + *_h
HCOO_s + H_h ↔ HCOO-H_s + *_h → HCOOH_g + *_s + *_h

Table S3. Electronic formation energies and vibrational frequencies of adsorbents on the Fe-based surfaces

Surface name	Site name	Species name	Formation energy	Frequencies
None	gas	HCOOH	2.437	[3614, 2985, 1731, 1377, 1259, 1043, 1001, 672, 602]
None	gas	C_2H_6	0.812	[3929, 3026, 3000, 2955, 2947, 2825, 2142, 1496, 1472, 1403, 1389, 1381, 1007, 958, 810, 771, 339, 253]
None	gas	C_2H_4	2.316	[3152, 3122, 3070, 3059, 1640, 1458, 1358, 1224, 1041, 948, 935, 823]
None	gas	C_2H_2	4.348	[3415, 3319, 1994, 767, 765, 618]
None	gas	CH_4	0.000	[3450, 3333, 2963, 2801, 2151, 1703, 1272, 502, 242]
None	gas	H_2	0.000	[4422]
None	gas	CO	2.695	[2099]
None	gas	CO_2	2.779	[2311, 1291, 621, 618]
None	gas	H_2O	0.000	[3780, 3694, 1614]
None	gas	O_2	5.825	[1495]
Fe	110	CO	1.184	[1858, 416, 412, 405, 127, 122]
Fe	110	CO_2	2.007	[1535, 1080, 659, 405, 271, 176, 110, 81, 53]
Fe	110	O	-0.719	[396, 383, 219]
Fe	110	H	-0.503	[1028, 787, 587]
Fe	110	HCOO	1.261	[2994, 1443, 1328, 1274, 956, 732, 326, 274, 252, 140, 131, 90]
Fe	110	COOH	1.884	[3508, 1296, 1149, 1005, 637, 596, 411, 293, 243, 126, 108, 62]
Fe	110	OH	-0.711	[3651, 595, 542, 328, 229, 217]

Fe	110	CHO	1.392	[2924, 1178, 868, 651, 464, 315, 263, 243, 166]
Fe	110	O-H	0.272	[1130, 700, 420, 296, 38]
Fe	110	H-OH	0.778	[3438, 1593, 1139, 718, 507, 410, 186, 164, 96]
Fe	110	CO-O	2.643	[1663, 621, 387, 329, 314, 238, 187, 131, 102]
Fe	110	COO-H	2.906	[1358, 1114, 1054, 681, 553, 380, 296, 248, 161, 86, 67]
Fe	110	H-COO	2.472	[2689, 1604, 1320, 999, 917, 686, 239, 188, 174, 162, 149, 101]
Fe	110	CO-OH	2.576	[3508, 1351, 1167, 899, 598, 552, 389, 255, 198, 102, 84, 67]
Fe	110	H-COOH	2.589	[3614, 2985, 1731, 1377, 1259, 1043, 1001, 672, 602]
Fe	110	HCOO-H	3.103	[3614, 2985, 1731, 1377, 1259, 1043, 1001, 672, 602]
Fe	110	H-CO	1.826	[2924, 1178, 868, 651, 464, 315, 263, 243, 166]
Fe	110	HCO-O	2.308	[2994, 1443, 1328, 1274, 956, 732, 326, 274, 252, 140, 131, 90]
Fe_3C	001	CO	1.154	
Fe_3C	001	CO_2	1.839	
Fe_3C	001	O	-0.644	
Fe_3C	001	H	-0.578	
Fe_3C	001	HCOO	1.190	
Fe_3C	001	COOH	1.858	
Fe_3C	001	OH	-0.801	
Fe_3C	001	CHO	1.403	
Fe_3C	001	O-H	0.209	
Fe_3C	001	H-OH	0.730	

Fe_3C	001	CO-O	2.567
Fe_3C	001	COO-H	2.817
Fe_3C	001	H-COO	2.261
Fe_3C	001	CO-OH	2.510
Fe_3C	001	H-COOH	2.507
Fe_3C	001	HCOO-H	3.061
Fe_3C	001	H-CO	1.742
Fe_3C	001	HCO-O	2.305
Fe_5C_2	001	CO	1.351
Fe_5C_2	001	CO_2	1.863
Fe_5C_2	001	O	-0.319
Fe_5C_2	001	H	-0.395
Fe_5C_2	001	HCOO	0.834
Fe_5C_2	001	COOH	1.883
Fe_5C_2	001	OH	-0.661
Fe_5C_2	001	CHO	1.861
Fe_5C_2	001	O-H	0.457
Fe_5C_2	001	H-OH	0.825
Fe_5C_2	001	CO-O	2.806
Fe_5C_2	001	COO-H	2.895
Fe_5C_2	001	H-COO	2.363
Fe_5C_2	001	CO-OH	2.670
Fe_5C_2	001	H-COOH	2.677
Fe_5C_2	001	HCOO-H	3.012
Fe_5C_2	001	H-CO	2.137
Fe_5C_2	001	HCO-O	2.440
v_Fe_3O_4	111	CO	0.873
v_Fe_3O_4	111	CO_2	1.222
v_Fe_3O_4	111	H	-0.769
v_Fe_3O_4	111	COOH	2.261
v_Fe_3O_4	111	OH	-1.233
v_Fe_3O_4	111	O	-0.621

Fe-K	110	CO	0.969
Fe-K	110	CO_2	1.500
Fe-K	110	O	-0.867
Fe-K	110	H	-0.492
Fe-K	110	HCOO	1.055
Fe-K	110	COOH	1.693
Fe-K	110	OH	-0.632
FeCu	110	CO	1.338
FeCu	110	CO_2	2.108
FeCu	110	O	-0.272
FeCu	110	H	-0.271
FeCu	110	HCOO	1.176
FeCu	110	COOH	2.142
FeCu	110	OH	-0.454
FeCu-K	110	CO	1.008
FeCu-K	110	CO_2	1.607
FeCu-K	110	O	-0.592
FeCu-K	110	H	-0.351
FeCu-K	110	HCOO	0.905
FeCu-K	110	COOH	1.900
FeCu-K	110	OH	-0.711
Fe-K_2O	110	CO_2	1.022
Fe-K_2O	110	OH	-0.517
FeCu-K_2O	110	CO_2	1.166
FeCu-K_2O	110	OH	-0.369
Fe_2O_3	001	CO	1.523
Fe_2O_3	001	CO_2	1.289
Fe_2O_3	001	O	0.538
Fe_2O_3	001	H	0.207
Fe_2O_3	001	HCOO	1.453
Fe_2O_3	001	COOH	1.405
Fe_2O_3	001	OH	-0.141

Fe_2O_3	001	CHO	1.762
Fe_2O_3	001	O-H	1.251
Fe_2O_3	001	H-OH	1.152
Fe_2O_3	001	CO-O	2.923
Fe_2O_3	001	COO-H	2.565
Fe_2O_3	001	H-COO	2.501
Fe_2O_3	001	CO-OH	2.696
Fe_2O_3	001	H-COOH	2.778
Fe_2O_3	001	HCOO-H	3.359
Fe_2O_3	001	H-CO	2.749
Fe_2O_3	001	HCO-O	3.119
Fe_3O_4	111	CO	1.286
Fe_3O_4	111	CO_2	1.411
Fe_3O_4	111	O	0.246
Fe_3O_4	111	H	0.187
Fe_3O_4	111	HCOO	0.899
Fe_3O_4	111	COOH	2.002
Fe_3O_4	111	OH	-0.508
Fe_3O_4	111	CHO	1.054
Fe_3O_4	111	O-H	0.900
Fe_3O_4	111	H-OH	1.039
Fe_3O_4	111	CO-O	2.764
Fe_3O_4	111	COO-H	3.017
Fe_3O_4	111	H-COO	2.481
Fe_3O_4	111	CO-OH	2.776
Fe_3O_4	111	H-COOH	3.248
Fe_3O_4	111	HCOO-H	3.196
Fe_3O_4	111	H-CO	2.408
Fe_3O_4	111	HCO-O	2.373
v_Fe_5C_2	111	CO	1.074
v_Fe_5C_2	111	CO_2	1.482
v_Fe_5C_2	111	O	-0.493

v_Fe_5C_2	111	OH	-0.693
Cu-Fe_3O_4	111	CO	1.204
Cu-Fe_3O_4	111	CO_2	1.520
Cu-Fe_3O_4	111	OH	-0.331
Cu-Fe_3O_4	111	O	0.328
Co-Fe_3O_4	111	CO_2	1.051
Co-Fe_3O_4	111	OH	-0.703
Cr-Fe_3O_4	111	CO_2	1.841
Cr-Fe_3O_4	111	OH	-0.418
Mn-Fe_3O_4	111	CO_2	1.394
Mn-Fe_3O_4	111	OH	-1.376
Ni-Fe_3O_4	111	CO_2	2.272
Ni-Fe_3O_4	111	OH	-0.059
V-Fe_3O_4	111	CO_2	2.023
V-Fe_3O_4	111	OH	-0.432
Zn-Fe_3O_4	111	CO_2	1.672
Zn-Fe_3O_4	111	OH	-0.391

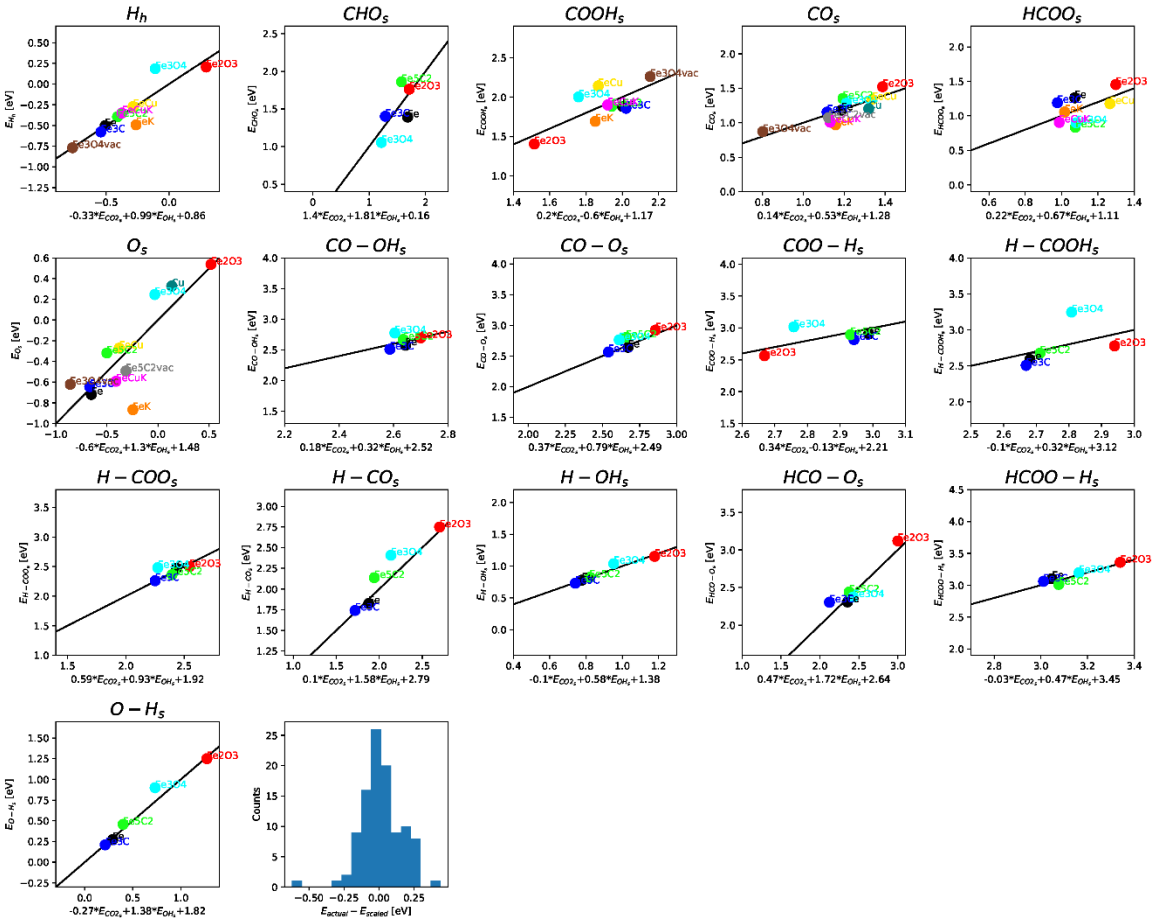

Figure S4. Formation energies of intermediates and transition states, plotted as a function of CO_2* formation energy (E_{CO2}) and OH* formation energy (E_{OH}). Scaling parameters are given below the plots.

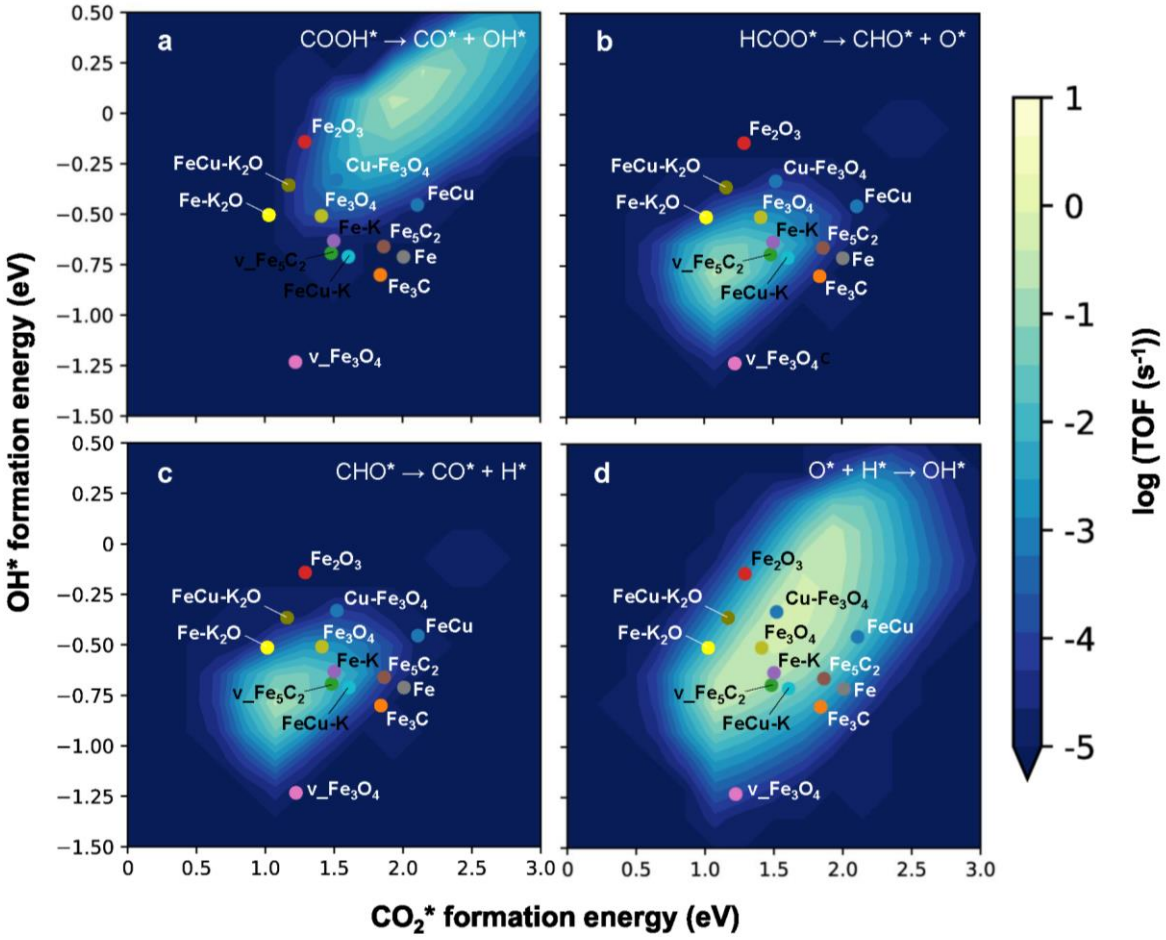

Figure S5. Rate volcano plots for elementary reaction steps in RWGS reaction, plotted as a function of the descriptors, CO_2* formation energy and OH* formation energy. T = 300 °C and P = 2.5 MPa.

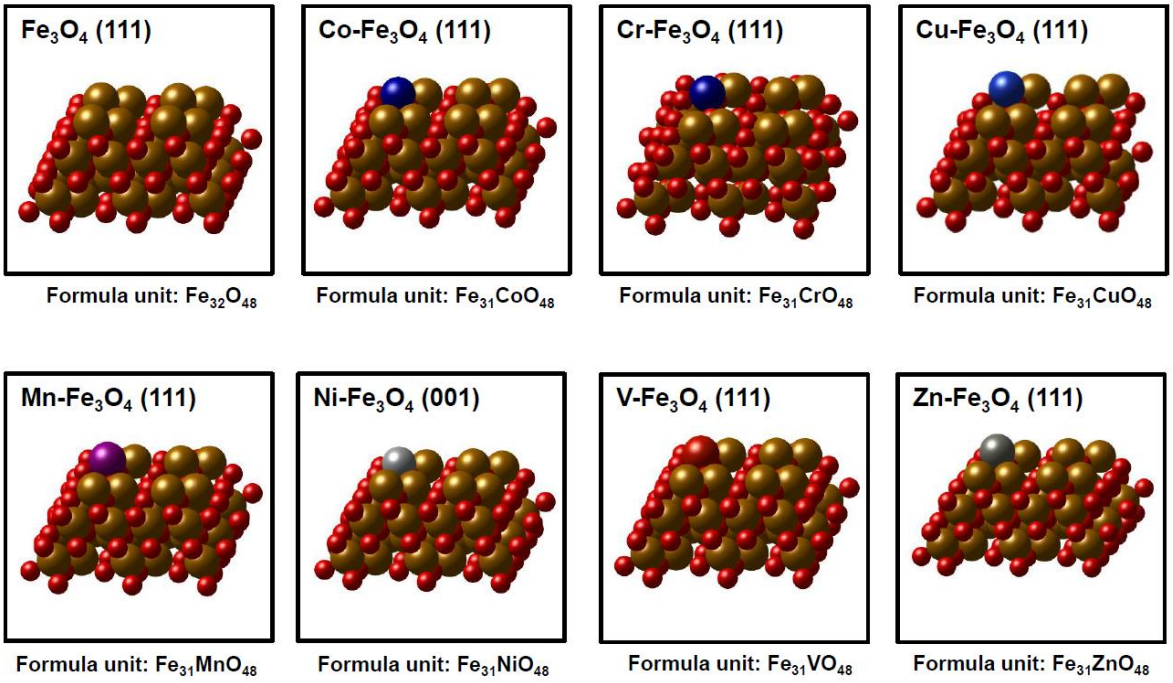

Figure S6. The optimized unit cell structures of Fe_3O_4 (111) and Me-Fe_3O_4 (111) surfaces. In the Me-Fe_3O_4 surfaces, element of Fe_{oct2} site is substituted by V, Cr, Mn, Fe, Co, Ni, Cu, and Zn.

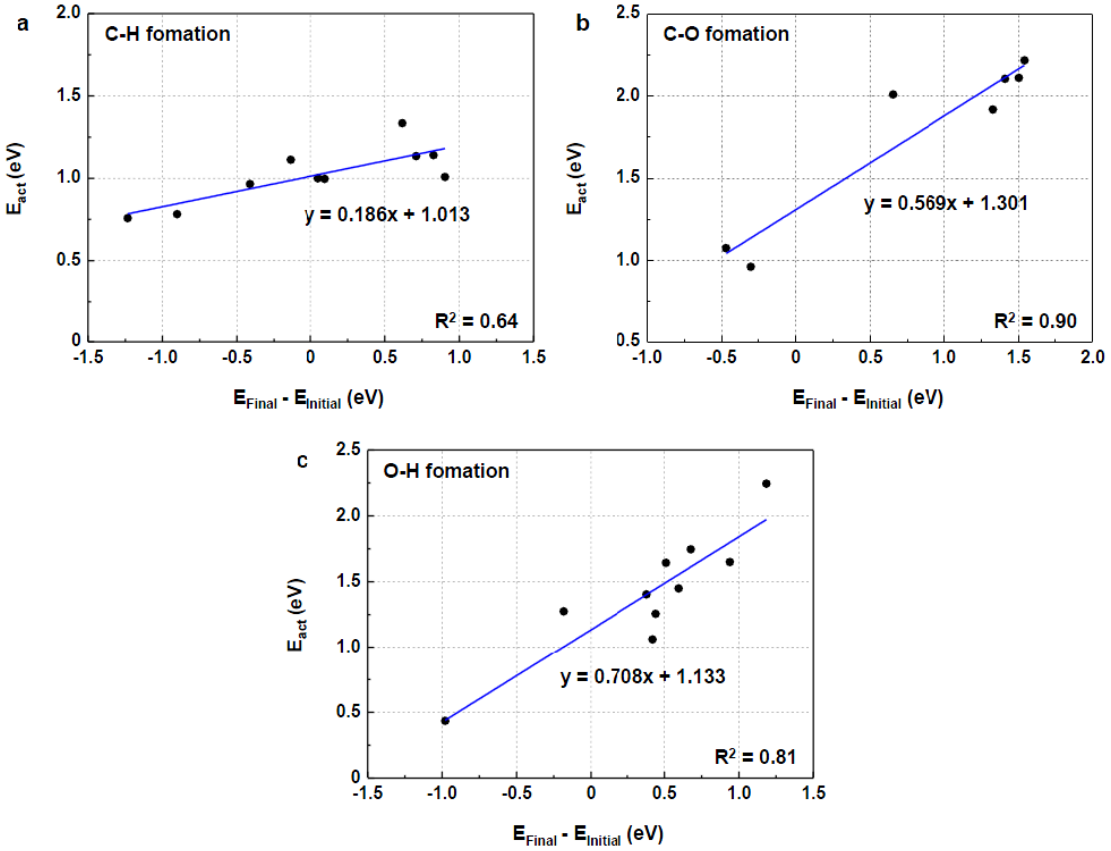

Figure S7. Bell–Evans–Polanyi correlations for (a) C-H bond, (b) C-O bond, and (c) O-H bond formation steps on Fe-based surfaces.

Table S4. Self-interaction parameters for Fe (110) surface.

Surface	Adsorbents	Self-interaction parameter
Fe	CO_2	8.549
Fe	CO	2.106
Fe	O	6.018
Fe	HCOO	4.699
Fe	COOH	9.012
Fe	OH	3.177
Fe	CHO	3.195

Table S5. Verification of self-interaction parameters by comparing E_{DFT}[a] and E_{est}[b] at 0.375 ML.

Adsorbate	CO_2*	CHO*	O*	OH*
E_{DFT} (eV)	1.947	1.349	-0.720	-0.767
E_{est} (eV)	1.870	1.366	-0.802	-0.807
E_{diff} (eV) [c]	0.077	0.017	0.082	0.040

[a] Electronic formation energy at 0.375 ML calculated from DFT calculation.

[b] Electronic formation energy at 0.375 ML predicted using interaction parameters.

[c] $E_{diff} = |E_{DFT} - E_{est}|$

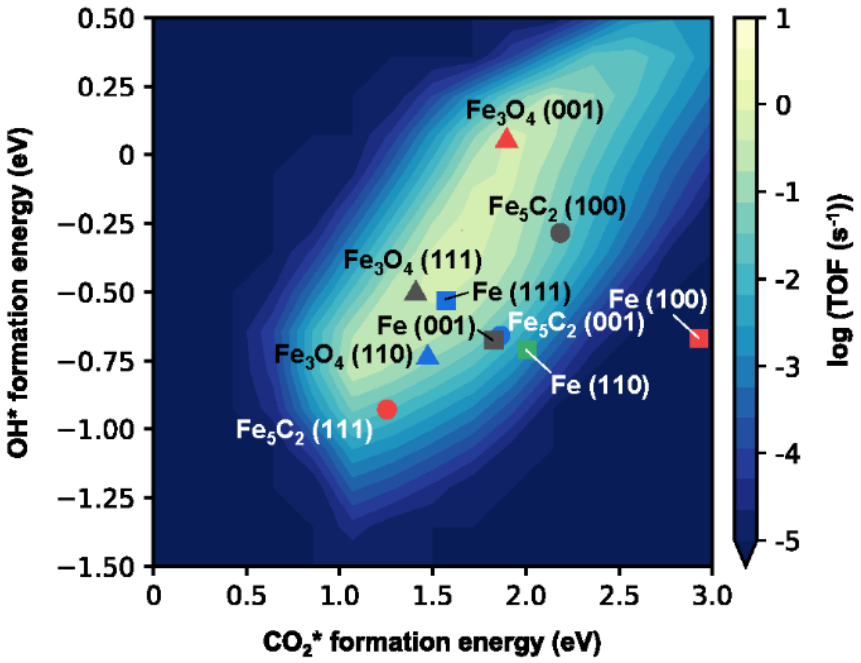

Figure S8. CO production rates over Fe (square), Fe_5C_2 (circle), and Fe_3O_4 (triangle) surfaces with various facets plotted as a function of the CO_2* and OH* formation energies. T = 300 °C and P = 2.5 MPa.